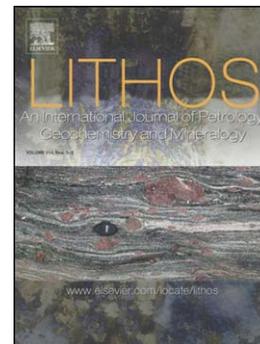# Accepted Manuscript

Reconstruction of magmatic variables governing recent Etnean eruptions: Constraints from mineral chemistry and P-T-fO$_2$-H$_2$O modelling

S. Mollo, P.P. Giacomoni, M. Coltorti, C. Ferlito, G. Iezzi, P. Scarlato

Please cite this article as: Mollo, S., Giacomoni, P.P., Coltorti, M., Ferlito, C., Iezzi, G., Scarlato, P., Reconstruction of magmatic variables governing recent Etnean eruptions: Constraints from mineral chemistry and P-T-fO$_2$-H$_2$O modelling, *LITHOS* (2014), doi: 10.1016/j.lithos.2014.11.020

Reconstruction of magmatic variables governing recent Etnean eruptions: constraints from mineral chemistry and P-T-fO$_2$-H$_2$O modelling

S. Mollo[1], P.P. Giacomoni[2], M. Coltorti[2], C. Ferlito[3], G. Iezzi[1,4], P. Scarlato[1]

[1]Istituto Nazionale di Geofisica e Vulcanologia, Via di Vigna Murata 605, 00143 Roma, Italy

[2]Dipartimento di Fisica e Science della Terra, Università di Ferrara, Via Saragat 1, 44122 Ferrara, Italy

[3]Dipartimento di Scienze Biologiche, Geologiche e Ambientali, Università di Catania, Via A. Longo 19, 95125Catania, Italy

[4]Dipartimento di Ingegneria & Geologia, Università G. d'Annunzio, Via Dei Vestini 30, 66013 Chieti, Italy

Corresponding author:

Silvio Mollo

Istituto Nazionale di Geofisica e Vulcanologia

Via di Vigna Murata 605

00143 ROMA - ITALY

office tel.   +39 0651860674

fax   +39 0651860507

e-mail   mollo@ingv.it

Abstract

Petrological investigations of active volcanoes are often supported by mass balances, thermodynamic calculations and/or experiments performed at key conditions. Conversely, the compositions of mineral phases found in natural products are generally used as input data for predictive models calibrated to derive the intensive variables of the magmatic system. In order to evaluate the extent to which mineral chemistry records crystallization conditions, we have compared the compositions of olivine, clinopyroxene, plagioclase and titanomagnetite in 2001-2012 trachybasaltic lavas at Mt. Etna with those obtained through thermodynamic simulations and experiments conducted under anhydrous, water-undersaturated and water-saturated conditions. This systematic comparison allows us to track recent differentiation processes beneath Mt. Etna, as well as the P-T-fO$_2$-H$_2$O variables controlling the solidification path of magma. Two compositionally distinct populations of olivine and clinopyroxene phenocrysts are found in these lavas: Mg-rich and Mg-poor minerals formed at 600-1100 MPa and 1100-1250 °C, and 0.1-500 MPa and 1050-1175 °C, respectively. The oxygen fugacity varies by 1-2 log units suggesting water exsolution during magma ascent in the conduit and magma emplacement near the surface. The nucleation and growth of normally zoned plagioclases occurs at P <100 MPa, when the amount of H$_2$O dissolved in the melt abruptly decreases from about 3.0 to 0.2 wt.% due to magma decompression and degassing. This leads to the conclusion that Etnean magmas fractionate throughout the entire length of the vertically developed plumbing system where magma mixing, volatile exsolution and degassing are the most important processes driving eruptions.

1. Introduction

Mt. Etna volcano (Sicily, Italy) is the largest volcano in Europe and one of the most active volcanoes on Earth. The onset of volcanism occurred with the eruption of tholeiitic basalts (ca. 500 ka) and, subsequently, the composition of magmas shifted towards a more alkaline affinity (ca. 220 ka) (Tanguy et al., 1997). Compared with the oldest historical eruptions, the degassing rate, the concentration of alkaline elements and the radiogenic strontium significantly increased in the last four decades (Armienti et al., 2004; Corsaro et al., 2007). A distinctive feature of this recent activity is the relatively constant degree of magmatic differentiation characterized by the eruption of trachybasaltic lavas with a uniform phenocryst assemblage of olivine, clinopyroxene, plagioclase, and titanomagnetite (Corsaro et al., 2009). The overall composition of phenocrysts is controlled by several processes that occur in (1) the deepest parts of the plumbing system during magma segregation at mantle depths (Armienti et al., 2007, 2013; Viccaro and Cristofolini, 2008), (2) at shallow crustal levels where magma differentiation, mixing and degassing are active processes (Ferlito et al., 2011; Lanzafame et al. 2013; Corsaro et al., 2013; Giacomoni et al., 2014) and (3) the emplacement conditions including the effect of cooling rate (Mollo et al., 2011a, 2013a; Scarlato et al., 2014).

Detailed petrological and geochemical studies have suggested that the plumbing system at Mt. Etna is governed by frequent inputs from mantle depths of primitive, volatile-rich magmas that mix with more evolved, degassed melts residing at shallow crustal levels (Clocchiatti et al., 2004; Metrich et al., 2004; Spilliaert et al., 2006; Ferlito et al., 2008; Corsaro et al., 2013). For the case of 2006 summit eruptive episodes, the history tracked by olivine crystals reveals that the magma pathway within the shallow plumbing system is controlled by two mafic recharge events within a few months where magma supply triggered the onset of a distinct eruptive cycle (Khal et al., 2011).

Despite the fact that the isotope signature of some lavas reveals heterogeneities in the mantle source, both primitive and more differentiated magmas are systematically buffered to the composition of trachybasalt in terms of major element compositions due to the continuous supply of

magma from the mantle (Ferlito and Lanzafame, 2012; Ferlito et al., 2014; Giacomoni et al., 2014). Thus whole-rock geochemistry alone is unable to comprehensively track the ascent paths of Etnean magmas. Workers primarily relying on mass balance calculations have proposed different petrogenetic mechanisms to explain the evolution of magmas, leading to number of controversies that are still matter of debate. Michaud (1995) proposed a mobility of crustal components (i.e., K, Rb and Cs) and their selective contamination of the magma as a consequence of the percolation of a carrier fluid phase through the upper parts of the magmatic feeding system. In contrast, Schiano et al. (2004) suggested that the geochemical evolution of Etnean magmas is due to a progressive transition from a predominantly intraplate-type mantle source to a different one contaminated by slab-derived fluids originated by the progressive southward migration of the slab or continuous opening of a slab window. Recently, Ferlito and Lanzafame (2010) argued that supercritical fluids coming from deeper magmas from the mantle carrying alkali Cl-complexes migrate through basic to intermediate magmas residing in the shallow feeding system. As chlorine exsolves and leaves the system, alkalis are released contributing to the observed potassium enrichment of magmas erupted after 1971.

These different petrogenetic models highlight a general paucity of information on the crystallization conditions of magma. While whole-rock data and mineral compositions are frequently documented and discussed, lesser importance has been given to their significance for the evolution of magma at both pre-eruptive and syn-eruptive conditions (Mollo et al., 2011b, 2013b). Specifically, the limited inter-crystal compositional variations recorded in the cores of larger phenocrysts hosted in lavas indicate a pristine equilibrium at nearly-static crystallization conditions. In contrast, the complex compositions of phenocryst mantles and rims, as well as those of micro-phenocrysts and microlites, mainly reflects disequilibrium crystallization under dynamic conditions due to magma mixing, rapid decompression and/or cooling during magma ascent in the conduit and lava flowage (Viccaro et al., 2010; Corsaro et al., 2013; Mollo et al., 2013b; Lanzafame et al., 2013; Applegarth et al., 2013). In order to decipher the pre-eruptive conditions of recent Etnean magmas

and track their P-T-fO$_2$-H$_2$O paths, we have compared the compositions of phenocrysts found in 2001-2012 lavas with those obtained through phase equilibrium experiments and thermodynamic simulations conducted over a wide range of crystallization conditions. The crystallization conditions gained through this comparison have been integrated with the estimation of intensive magmatic variables through mineral-melt equilibrium models, thermometers, barometers, oxygen barometers, and hygrometers. Our predictions contribute to a reconciliation of most of the contradictions raised during an intense debate with regards to magma mixing, water exsolution and degassing processes operating from the mantle to the shallow feeding system to the summit crater of Mt. Etna volcano.

2. Experiments and analyses

For the purpose of this study, we have compiled three distinct datasets comprising natural, experimental and thermodynamic compositions of olivine, clinopyroxene, plagioclase, and titanomagnetite. Natural and experimental datasets from the literature have been integrated with new data from this study in order to increase the statistical significance of natural compositions and to extend the intervals of crystallization conditions reproduced in laboratory. Both experiments and analyses were conducted at the HP-HT Laboratory of Experimental Volcanology and Geophysics of the Istituto Nazionale di Geofisica e Vulcanologia (INGV) in Rome, Italy. These datasets are reported in the Excel spreadsheet provided as supplementary material together with whole-rock analyses.

The starting material used for the experiments is a trachybasalt from the 2012 eruption at Mt. Etna. In order to saturate the sample holders in iron, some aliquots of the powdered rock were loaded into the Pt crucible and Pt capsules, and run for 3 h at 1600 °C in an atmosphere chamber furnace. They were then quenched and cleaned in a hot HF solution. In this way, the iron loss from the samples during the experiments was kept to ≤5 % of the initial amount (see Mollo et al., 2013b). The starting glass was produced by double melting in the Pt crucible 20 g of powdered rock at 1600 °C and atmospheric pressure for 30 min. The glass was analyzed by X-ray powder diffraction

and scanning electron microscopy, and no crystalline phases were detected. The starting glass composition is reported in the supplementary material. Pressure experiments were performed at 250 and 400 MPa in a piston cylinder apparatus. Pt capsules loaded with the powdered glass were positioned into a 19.1-mm NaCl–crushable alumina–pyrophyllite–pyrex assembly which produced a fO$_2$ of NNO+1.5 (see Mollo et al. 2013d). Water was added by microsyringe into the charge so that hydrous experiments contained 1, 1.5, and 2 wt.% H$_2$O. The charges were heated directly to the target temperatures of 1000, 1070, 1100, 1130, and 1150 °C that were maintained constant for 24 h. Each experiment was rapidly quenched using a quench rate of 2000 °C/min. The run product was mounted in epoxy and a polished thin section was produced from the epoxy block.

Microprobe analyses were carried out with a Jeol-JXA8200 equipped with five spectrometers. The analyses were conducted on both experimental phases and natural samples from 2001-2012 eruptions. For glasses, a slightly defocused electron beam with a size of 3 μm was used with a counting time of 5 s on background and 15 s on peak. For crystals, the beam size was 1 μm with a counting time of 20 and 10 s on peaks and background, respectively. The following standards have been adopted for the various chemical elements: jadeite (Si and Na), corundum (Al), forsterite (Mg), andradite (Fe), rutile (Ti), orthoclase (K), barite (Ba), apatite (P), spessartine (Mn) and chromite (Cr). Sodium and potassium were analyzed first to prevent alkali migration effects. The precision of the microprobe was measured through the analysis of well-characterized synthetic oxides and minerals. Data quality was ensured by analyzing these test materials as unknowns. Based on counting statistics, analytical uncertainties relative to their reported concentrations indicate that precision was better than 5% for all cations.

3. Results

3.1. *Natural dataset*

The natural dataset consists of phenocryst compositions from trachybasaltic lavas erupted during 2001-2012 magmatic activity (Spilliaert et al., 2006; Corsaro et al., 2007; Viccaro et al.,

2006, 2010; Nicotra and Viccaro, 2012; Collins et al., 2013; Giacomoni et al., 2014), and also comprises new data from this study.

Olivine shows compositions from Fo_{67} to Fo_{88} that are generally negatively correlated with the amount of Ca (Fig. 1a). The Mg# [Mg# = atomic $Mg/(Mg+Fe^{2+})$] of clinopyroxene changes from 54 to 85 clustering over two distinct compositional intervals of $Mg\#_{54-74}$ and $Mg\#_{75-85}$ (Fig. 1b); conversely, no clear variations are observed for Ti ranging from 0.02 to 0.07 apfu. The content of An (anorthite) in plagioclase varies widely from 56 to 89 but the amount of Fe remains almost constant with values of 0.1-0.4 apfu (Fig. 1c). Most titanomagnetite phenocrysts lie between Usp_{25} and Usp_{44} (ulvospinel) and only a few data show higher Usp_{48-55} values corresponding to low Al+Mg contents (Fig. 1d).

These phenocrysts are hosted in lavas showing almost homogeneous whole-rock compositions. The analyses indicate a limited variation for both SiO_2 and Na_2O+K_2O that are in the range of 47-51 wt.% and 5-6 wt.%, respectively. This implies that magmas are buffered to the composition of a trachybasalt with $Mg\#_{47-57}$.

3.2. Experimental dataset

The experimental dataset consists of the compositions of crystals formed under anhydrous, water-undersaturated and water-saturated conditions. Water-saturated experiments were conducted by Metrich and Rutherford (1998) between 1009 and 1135 °C, for $P_{H2O} = P_{total}$ varying from 27 to 120 MPa under G-CH, QFM and NNO buffering conditions. Anhydrous and water-undersaturated phase equilibrium data were obtained at 1000-1130 °C, 0.1-500 MPa, 0-2.8 wt.% H_2O, and NNO-NNO+1.5 buffer by Dolfi and Trigila (1983) and Mollo et al. (2010, 2011b, 2013b, 2013c), also comprising new data from this study.

The crystallization of olivine occurs only in water-saturated runs where olivine is the first phase on liquidus. Conversely, clinopyroxene is the liquidus phase in anhydrous and water-undersaturated runs. The Fo content in olivine changes from 67 to 81 (Fig. 1a) and it is positively

correlated with P_{H2O} as documented by Metrich and Rutherford (1998). Clinopyroxenes from water-undersaturated experiments show $Mg\#_{52-69}$ compositions, whereas more primitive $Mg\#_{70-80}$ crystals are found in anhydrous and water-saturated runs (Fig. 1b). The An content in plagioclase is strongly influenced by H_2O with An_{55-64} compositions in anhydrous and water-undersaturated runs, and An_{71-89} compositions in water-saturated experiments (Fig. 1c). The amount of Usp component in titanomagnetites from water-saturated experiments is generally lower than that measured under anhydrous and water-saturated conditions (Fig. 1d).

3.3. MELTS dataset

The thermodynamic dataset has been calculated through MELTS (Ghiorso and Sack, 1995) simulations conducted on (1) a trachybasaltic composition representative of magmas most frequently sampled in the last decades (47.66 wt.% SiO_2, 5.68 wt.% Na_2O+K_2O, and $Mg\#_{50}$) and (2) the most primitive basalt ever sampled at Mt. Etna during the paroxysmal activity of the Mt. Maletto cone (47.29 wt.% SiO_2, 4.10 wt.% Na_2O+K_2O, and $Mg\#_{63}$). Thermodynamic runs started from the liquidus temperature and continued along an equilibrium crystallization path terminated at 1050 °C. The pressure, melt-water content and oxygen fugacity were varied from 100 to 400 MPa, from 1 to 2 wt.% H_2O, and from NNO to NNO+1.5 buffers, respectively, in agreement with the plumbing system conditions suggested by previous authors (Armienti et al., 1994a, Mollo et al., 2011a, Collins et al., 2013, Giacomoni et al., 2014) to guarantee a stable phase assemblage of olivine, clinopyroxene, plagioclase and titanomagnetite.

The Fo content in olivine ranges from 67 to 83 with increasing H_2O and MgO in the starting melt (Fig. 1a). The same applies to the composition of clinopyroxene showing Mg# between 56 and 66 (Fig. 1b). However, the most mafic populations of clinopyroxene and olivine phenocrysts are not reproduced in full by MELTS- and experimentally-derived compositions, suggesting equilibrium with magmas more primitive than the Mt. Maletto basalt (i.e., Mg# > 63; see below). An in

plagioclase varies widely from 45 to 80 (Fig. 1c). The Usp component in titanomagnetite increases from 21 to 39 paralleling Al+Mg enrichments (Fig. 1d).

MELTS simulations conducted on the Mg#$_{50}$ starting composition indicate that olivine (Fo$_{73-77}$) is subordinated to the early formation of clinopyroxene at 400 MPa (Fig. 2a). The stability field of olivine expands at the expense of plagioclase as the amount of water increases from 1 to 2 wt.%. At 100 MPa, olivine (Fo$_{79-80}$) is the liquidus phase followed by the formation of clinopyroxene, plagioclase and titanomagnetite (Fig. 2b). For the more primitive Mg#$_{63}$ starting composition, MELTS simulations at 400 MPa show that olivine (Fo$_{81-85}$) replaces clinopyroxene as the liquidus phase when the amount of water increases from 1 to 2 wt. % (Fig. 2c). At 100 MPa, olivine (Fo$_{80-81}$) is always the liquidus phase irrespective of the melt-water content (Fig. 2d). However, the effect of this low pressure is that plagioclase oversteps the formation of clinopyroxene with decreasing water concentration (Fig. 2d). On the whole, a phase assemblage comprising olivine, clinopyroxene and plagioclase is achieved at degrees of fractionation between 10 and 20 wt.%. Titanomagnetite occurs at late stages of differentiation and its stability field decreases with increasing pressure and melt-water concentration.

3.4. Testing for equilibrium

To test whether natural clinopyroxene phenocrysts are in equilibrium with their host magma, we have adopted the model of Mollo et al. (2013b) based on the difference (Δ) between diopside+hedenbergite (DiHd) components predicted for clinopyroxene via regression analysis of clinopyroxene-melt pairs in equilibrium conditions, and those measured in the analyzed crystals. This model has been successfully tested when multiple discrete populations of clinopyroxene are found in the same volcanic units (Mollo and Masotta, 2014). Under such circumstances, near equilibrium crystallization conditions are achieved when the clinopyroxene compositions plot within 10% of the one-to-one equilibrium line corresponding to values of ΔDiHd ≤0.1 (Jeffery et al., 2013). Clinopyroxene-melt equilibrium modelling confirms the occurrence of two distinct

clinopyroxene populations distributed over low (54-74) and high (75-85) values of Mg# (Fig. 3a). Near-equilibrium crystallization conditions are observed between Mg#$_{54-74}$ phenocrysts and recent trachybasaltic lavas, whereas Mg#$_{75-85}$ clinopyroxenes suggest crystallization with more primitive magmas like the basaltic composition of Mt. Maletto (Fig. 3a).

The equilibrium crystallization of plagioclase phenocrysts has been tested through the Ab–An exchange reaction proposed by Putirka (2008). The equilibrium constant is constrained within two temperature-dependent intervals of $^{plg–melt}Kd_{Ab–An} = 0.10 \pm 0.05$ at T <1050 °C and $^{plg–melt}Kd_{Ab–An} = 0.27 \pm 0.11$ at T >1050 °C. Our estimates indicate that the two phenocryst populations to the extremes of the plagioclase evolutionary trend (An$_{60-65}$ and An$_{81-88}$) are in disequilibrium with the host magma (Fig. 3b). Conversely, most of $^{plg–melt}Kd_{Ab–An}$ values calculated for Etnean plagioclases correspond to the equilibrium range of 0.27 ± 0.11. Therefore, the thermal path experienced by magma during plagioclase formation lies between the initial saturation temperature of plagioclase and the closure temperature of crystal growth corresponding to values higher than 1050 °C.

By means of equilibrium compositions recovered for clinopyroxenes and plagioclases found in the same host lava, we have estimated the redox state of the melt using the oxygen barometer of France et al., (2010). The method of propagation of errors was used to determine how replicated analyses determined the uncertainty in the resulting fO$_2$ estimates. The oxygen barometer is primarily based on the different partitioning behaviour of ferrous and ferric iron between minerals and the melt. Plagioclase incorporates more Fe^{3+} than Fe^{2+}, while Fe^{2+} is more compatible in clinopyroxene than Fe^{3+}. The model of France et al. (2010) was also tested for alkaline rocks from Mt. Etna volcano yielding reliable estimates (Mollo et al., 2011a; Giacomoni et al., 2014). Results from plagioclase-clinopyroxene pairs indicate a redox state corresponding to the NNO+1 buffer with a standard deviation of ±0.8 (Fig. 3c), in agreement with the oxygen fugacity most frequently documented for Etnean magmas (Armienti et al., 1994a, 2004, 2013; Mollo et al., 2011a, 2013a; Giacomoni et al., 2014). Considering this buffering range, we have partitioned the total Fe of the host magma between Fe^{2+} and Fe^{3+}, in order to test the equilibrium crystallization of olivine through

the Fe-Mg exchange reaction of Kress and Carmichael (1991). The model is known to show only a small dependence on melt composition, temperature, pressure and fO_2, with an almost constant value of $^{ol-melt}Kd_{Fe-Mg} = 0.30\pm0.03$ (Roeder and Emslie, 1970). The input temperature used for the calculation corresponds to that predicted for each olivine phenocrysts (see below). Our determinations highlight that about 70% of Fo_{70-80} olivines are in equilibrium with their host $Mg\#_{47-57}$ lavas (Fig. 3d); in contrast, about 30% of Fo_{81-88} phenocrysts suggest equilibrium with less differentiated $Mg\#_{58-68}$ magmas that are comparable to those erupted during the activity of Mt. Maletto cone or even with more primitive compositions.

4. Discussion

4.1. Olivine and clinopyroxene crystallization conditions

While the crystallization of olivine is suppressed in experiments conducted under anhydrous and water-undersaturated conditions, olivine is the liquidus phase in water-saturated experiments with compositions progressively enriched in Fo with increasing P_{H2O}. According to the observations of Sisson and Grove (1993), the piercing points in the Fo-Di-An system expands both the olivine and clinopyroxene stability field at the expense of plagioclase. Although water-saturated experiments promote the crystallization of Fo-rich olivine, its composition does not fully reach the highest Fo_{84-88} values measured in natural phenocrysts (Fig. 1a). The highest Fo_{85} composition is obtained only by MELTS simulations conducted at 400 MPa when olivine occurs as the liquidus phase of the primitive Mt. Maletto basalt (Figs. 1a and 2c). This suggests that primitive phenocrysts should have equilibrated with $Mg\#_{58-68}$ magmas residing at high pressures and temperatures. To better constrain the crystallization conditions of olivine, we have used the mineral-melt liquidus association option of Petrolog3 calibrated on olivine-melt and clinopyroxene-melt equilibrium models (Danyushevsky and Plechov, 2011). The host magma was crystallized along different olivine+clinopyroxene cotectics so that Fo in olivine and Mg# of clinopyroxene predicted by the model were comparable to those observed in natural phenocrysts. Note that the equilibrium

condition for the Fe-Mg exchange between olivine (or clinopyroxene) and melt was satisfied over a range of values between 0.33 and 0.24, consequently, the error of pressure and temperature estimate corresponds to 27 °C and 220 MPa, respectively. Our predictions indicate that Fo_{81-88} olivines equilibrated with $Mg\#_{58-68}$ magmas at 650-1050 MPa and 1150-1250 °C (Fig. 4a-b). On the other hand, Fo_{70-80} olivines saturated the trachybasaltic magmas at 0.1-450 MPa and 1100-1150 °C (Fig. 4a-b) consistent with MELTS simulations at 100 MPa (Fig. 2b). Our estimates support the existence of at least two main reservoirs that are compositionally distinct and, importantly, provide pressure and temperature constrains on the crystallization, transport and mixing of olivine phenocrysts. This finding is also complementary to the observations by Kahal et al. (2011) suggesting that olivines in historical lavas at Mt. Etna can be attributed to a plumbing system consisting of multiple magmatic environments in which magma is transported and mixed before eruption. The gradual input of mafic and gas-rich magma into different segments of the plumbing system is also accompanied by a major increase in the measured CO_2/SO_2 gas signal (Kahal et al., 2013). This initial recharge can reactivate the system and promote mixing in the more evolved shallow section of the plumbing system. According to Armienti et al. (2013), the plumbing system at Mt. Etna is constantly buffered to the composition of a trachybasalt due to the continuous supply of primitive magmas that mix with more differentiated magmas residing at shallower crustal levels. This process seems to be controlled by the magma supply rate at depth, in which different segments of the plumbing system may host compositionally distinct magmas for a time that depends on the supply rate itself and on the P-T-X conditions of magmas (see also Armienti et al., 2007). In this frame, our data provide evidence of the occurrence of at least two distinct P-T intervals: a deeper one in which mantle derived melts are buffered to become trachybasalts at near equilibrium conditions, and a shallower one in which disequilibrium processes prevail.

Results from tests for equilibrium have also revealed the occurrence of two distinct clinopyroxene populations in equilibrium with primitive and more differentiated magmas (Fig. 3a). The crystallization temperatures have been calculated using the thermometer of Putirka et al. (1996)

which has the advantage of being pressure- and water-independent with a relatively low uncertainty of 25 °C. The crystallization pressures have been predicted by the barometer of Putirka (2008) that is completely independent of the melt composition with a standard error of estimate of 200 MPa. As a whole, $Mg\#_{75-85}$ and $Mg\#_{54-74}$ clinopyroxene populations formed along two different P-T paths corresponding to values of 600-1100 MPa and 1150-1225 °C (Fig. 4c), and 0.1-500 MPa and 1050-1175 °C (Fig. 4d), respectively. These results extend the P-T model of Armienti et al. (2013) for prehistoric and historical eruptions to the most recent activity of Mt. Etna. For 1991-1993 eruptions Armienti et al. (1994b) reported whole rock geochemical analyses of temporally spaced lava samples showing minor compositional variations over the short time range of eruption; indeed, constant values of $^{87}Sr/^{86}Sr = 0.7035$ and $^{143}Nd/^{144}Nd = 0.5128$ confirmed the eruption of magmas with the same compositions. On the other hand, considering the geodynamic setting of Mt. Etna magmatism, Armienti et al. (2007) interpreted the long-term Sr-Nd isotope variation during 1852-2004 eruptions as the result of mixing between a slightly depleted mantle source and a subduction-related fluid characterized by $^{87}Sr/^{86}Sr = 0.7080$ and $^{143}Nd/^{144}Nd = 0.5122$. This mixing process is within the range defined by the typical composition of altered oceanic crust and that assumed for the sediments derived from the crust of Calabrian arc. Importantly, Armienti et al. (2007) also identified distinct clinopyroxene populations through independent evidence based on crystal size distribution and isotope analyses. $^{87}Sr/^{86}Sr$ data reveal the nucleation and growth of clinopyroxene phenocrysts in isotopically distinct magmas due to the occurrence of clinopyroxene cores ($^{87}Sr/^{86}Sr = 0.7035$) in disequilibrium with the host lavas ($^{87}Sr/^{86}Sr = 0.7036$). These pronounced temporal sequences of clinopyroxene–whole-rock disequilibria are caused by the evolving isotopic composition of the mantle source and the rate of magma supply to the uppermost parts of the feeding system. In light of this, olivine and clinopyroxene phenocrysts found in recent lavas testify to magma mixing processes where Mg-rich phenocrysts are carried by deep-seated primitive magmas into more differentiated reservoirs at shallow crustal levels (Corsaro et al., 2009, 2013).

Significantly, seismological and ground deformation data evidence the existence of two main magma storage regions at 6-8 km and 9-18 km below the volcanic summit (Patanè et al., 2003).

4.2. Water exsolution and degassing-induced crystallization

A key parameter controlling the crystallization behaviour and ascent rate of magmas is the amount of water dissolved in the melt. In this study the melt-water content has been determined with the clinopyroxene-based model of Armienti et al. (2013) calibrated for Etnean magmas and with error of 0.5 wt.% H_2O. The input temperature used for the model was that calculated for each clinopyroxene phenocryst by the pressure- and H_2O-independent model of Putirka et al. (1996) (Fig. 4b-c). Results have been then compared with those reported by Armienti et al. (2013) (Fig. 5a). At P >400 MPa, the amount of water in equilibrium with clinopyroxene increases from about 1 to 4 wt.% likely due to the increasing crystallization of anhydrous Etnean minerals as it was suggested by Armienti et al. (2013) or, alternatively, due to the contribution of H_2O-rich fluids rising from depth along the open conduit system as argued by Ferlito et al. (2014). In contrast, at P ≤400 MPa, the melt-water content decreases from about 4 to 1.5 wt.% with decreasing pressure in response to a lower water solubility (Collins et al., 2013). Arrays of P-T estimates for the 2001-2006 eruptions indicate an acceleration of the ascent rate due to abundant loss of water in the shallower parts of the plumbing system (Armienti et al., 2013 and references therein). Volatile-rich magmas residing at pressures <100 MPa undergo strong degassing while travelling from the conduit onto the surface of Mt. Etna volcano (Metrich et al., 2004, Spilliaert et al., 2006; Collins et al., 2013). In the case of recent eruptions, the shallow plumbing system can be distinguished from a main storage region at depth where long-term mixing processes occur (Figs. 4 and 5a), and an upper conduit region in which magma differentiate under the effect of volatile exsolution and degassing.

To better understand the role played by water exsolution on crystal nucleation and growth at shallow crustal levels, we have used the An-Ab exchange between plagioclase and melt calibrated by Lange et al. (2009) that is a more precise hygrometer tool (0.32 wt.% of uncertainty) at low

pressure conditions. The amount of water dissolved in the melt during plagioclase crystallisation has been estimated by using An measured for normally zoned plagioclases (i.e., cores, mantles and rims) and the composition of the host magma (i.e., the trachybasalt whole-rock analysis). Each estimate has been conducted over a thermal range of 1050-1080 °C corresponding to direct measurements of inner lava flow temperatures (Tanguy and Clocchiatti, 1984). This restricted thermal range is consistent with (1) the equilibrium value of $^{plg-melt}Kd_{Ab-An}$ yielding temperatures higher than 1050 °C, (2) the crystallization temperature of Etnean plagioclase constrained experimentally (Metrich and Rutherford, 1998; Mollo et al., 2011b) and (3) the abundant syn-eruptive crystallization of plagioclase in lavas (Giacomoni et al., 2014 and references therein). Results show that the concentration of water in equilibrium with plagioclase phenocrysts decreases notably from 3.0 to 0.2 wt.% with decreasing An content (Fig. 5b). This trend is consistent with the loss-on-ignition of lava samples (0.13-2.8 wt.% LOI) and the lower melt-water content predicted by SolEx solubility program as the pressure decreases from 85 to 5 MPa (Witham et al., 2011); note that the concentration of CO_2 (0.1-0.4 wt.%), S (0.25-0.38 wt.%), and Cl (0.13-0.18 wt.%) frequently measured in trachybasaltic magmas were also used as input parameters for the solubility program (Metrich et al., 2004 and references therein). The Ab-An exchange observed during plagioclase evolution can be ascribed to water exsolution caused by the input of a CO_2-rich magma and/or CO_2 fluxing from depth. Melt inclusion studies found that one of the most primitive Etnean magmas is a basalt characteristically enriched in MgO (12.6 wt.%) showing the trace element signature of a garnet-bearing, metasomatized source (Kamenetsky and Clocchiatti, 1996; Kamenetsky et al., 2007). The high H_2O and CO_2 contents of the melt inclusion (3.8 and 0.33 wt.%, respectively) indicate prolonged permanence of the magma in a plumbing system undergoing intense volatile flushing (Ferlito et al., 2014). The fractionation of 10-15 wt.% of olivine shifts this primary basaltic composition towards that of Mt. Maletto magma which, in turn, preserves CO_2 concentrations close to the saturation level (Armienti et al., 2004). The continuous replenishment of deep-seated volatile-rich magmas during differentiation and degassing at shallow crustal levels can

reasonably control the volatile exsolution, decompression path, and crystallization behaviour of recent Etnean eruptions leading to CO_2/H_2O ratios that are remarkably higher than those expected for rapidly ascending magmas in a conventional open-degassing system (Spilliaert et al., 2006; Kamenetsky et al., 2007; Collins et al., 2009; Nicotra and Viccaro, 2012). For example, most olivine-hosted melt inclusions from the 2002 eruption were trapped between 220 and 170 MPa, defining a magma ponding zone at 5 ± 1 km b.s.l. (CO_2 = 700-1300 ppm and H_2O = 2.2-2.9 wt.%), affected by deep CO_2 flushing and consequent variable magma dehydration (Spilliaert et al., 2006). Water exsolution and degassing would also explain the oxygen fugacity change from 1 to 2 log units (Fig. 3c) (Metrich et al., 2004), consistent with works showing water-saturated magmas that are progressively more oxidized with increasing water in excess (Moore et al., 1995; Del Bello et al., 2014).

Although plagioclase phenocrysts show complex textures and compositions due to the combination of multiple processes (i.e., magma convection, mixing and degassing), there is growing recognition that plagioclase phenocryst cores equilibrated at depth whereas phenocryst mantles and rims as well as plagioclase microphenocrysts crystallized at syn-eruptive conditions during rapid magma decompression (Lanzafame et al., 2013; Giacomoni et al., 2014). Under such circumstances, the state of the system changed from H_2O-undersaturated to H_2O-saturated regimes driving the evolution of plagioclase. Therefore, An-rich cores testify to the onset of crystallization from H_2O-undersaturated, deep-seated magmas in equilibrium with almost constant water concentrations (Viccaro et al., 2010; Lanzafame et al., 2013). In contrast, the formation of compositionally intermediate mantles and more evolved rims indicate the stage of H_2O exsolution during magma decompression (Nicotra and Viccaro, 2012; Giacomoni et al., 2014). By means of textural analysis of natural and experimental data, Cashman (1993) documented that most Hawaiian basalts crystallize under conditions of heterogeneous nucleation, with the number density of pre-existing nucleii partially controlling textural responses to increasing degree of undercooling. In other words, plagioclase rims can heterogeneously nucleate on early-formed cores due to the shift in

the nucleation regime from homogeneous (near-equilibrium crystal growth in the magmatic reservoir) to heterogeneous (rapid crystal growth from the conduit to the surface) (Shea and Hammer, 2013; Iezzi et al., 2014). The rapid crystal growth of plagioclase at Mt. Etna is indicated by the entrapment of μm-sized melt embayments into the rims of coarse plagioclases likely due to fast volatile loss and strong undercooling (Brugger and Hammer, 2010 and references therein). In this view, anhydrous and water-undersaturated runs crystallize plagioclases with relatively low An contents reproducing the final stage of the solidification path of lavas and dikes at Mt. Etna rather than the onset of the crystallization in magmas (Fig. 1c). Conversely, the An content of plagioclase increases continuously with increasing H_2O and P_{H2O} (Moore and Carmichael, 1998) underscoring that An-rich crystals in water-saturated runs represent most of the natural phenocryst population, especially for An_{81-88} compositions that are not captured by the MELTS dataset (Fig. 1c). We emphasize that water-saturated experiments of Metrich and Rutherford (1998) were designed to investigate the effect of a degassing-driven crystallization due to the fast migration of H_2O-rich magmas at shallow depths. The system experienced little crystallization until H_2O started to exsolve in response to a water solubility decrease. The rapid separation of a H_2O-rich gas phase caused magma undercooling that promoted the nucleation and growth of plagioclases remarkably enriched in anorthite (Brugger and Hammer, 2010 and references therein). While MELTS calculations predict phase compositions at the thermodynamic equilibrium, a dynamically-controlled crystallization process due to rapid degassing is likely more appropriate to explain the high An_{81-88} contents measured in natural phenocrysts (Fig. 1c). Based on MELTS simulations, we conclude that these high An contents cannot be the result of melt-water concentrations >2 wt.% due to the enlargement of the stability field of olivine and clinopyroxene (Fig. 2). On the other hand, temperatures <1050 °C are energetically unfavourable for the incorporation of An into plagioclase, especially when the melt experiences high degrees of fractionation (>20 wt.%) and differentiation (MgO <4 wt.%) (Fig. 2). Therefore, it is not surprising that the $^{plg-melt}Kd_{Ab-An}$ model of Putirka

(2008) has faithfully identified An_{81-88} plagioclases as disequilibrium phenocrysts together with the more evolved An_{60-65} phenocrysts formed at the final stage of solidification (Fig. 3b).

Disequilibrium cation proportions are also observed for titanomagnetite phenocrysts showing Usp and Al+Mg contents different from those expected under equilibrium crystallization conditions (Spencer and Lindsley, 1981) (Fig. 1c). By means of geospeedometer calculations based on the different intra-crystal Ti-Al-Mg redistribution rates in titanomagnetite (Mollo et al., 2013d), we found that the majority of natural titanomagnetites formed under cooling paths of 1-8 °C/min testifying to rapid crystal growth conditions. Direct experimental observations conducted on pahoehoe trachybasaltic lava flows highlighted that the crystal- and volatile-rich nature of Etna products mostly reflects the rapid growth of plagioclase and titanomagnetite due to ascent times of 0.2-7 hours (Applegarth et al., 2013). On eruption, the phenocryst and microphenocryst content of lava flows is ≤50 wt.% but a great number of plagioclase and titanomagnetite crystals can still nucleate and grow by degassing- and cooling-driven crystallization mechanisms (Applegarth et al., 2013; Vetere et al., 2013; Iezzi et al., 2014). This is definitively demonstrated by MELTS data showing that 20 wt.% crystal fractionation shifts the original trachybasaltic magma toward MgO-poor compositions that are never erupted at Mt. Etna (Fig. 2a-b). Therefore, only a small amount of phenocrysts in Etnean lavas equilibrate at depth, while most of the crystallization is driven by the decompression path and cooling history of magma during its ascent in the conduit and emplacement to the surface (Lanzafame et al., 2013).

5. Conclusions

In this study, we highlighted the importance of mineral composition in deciphering magmatic processes at Mt. Etna employing a range of P-T-fO$_2$-H$_2$O models for multiple phases to better constrain the crystallization conditions of the plumbing system. The most important processes governing magma dynamics during 2001–2012 eruptions of Mt. Etna volcano are summarized in Fig. 6. Mg-rich olivine and clinopyroxene phenocrysts crystallize from deep-seated primitive

basalts at 600-1100 MPa and 1150-1250 °C (Fig. 6). Subsequently, these mafic phenocrysts are transported into shallow trachybasaltic reservoirs containing Mg-poor olivines and clinopyroxenes in equilibrium at 0.1-500 MPa and 1050-1175 °C (Fig. 6). Degassing-driven crystallization is the key mechanism controlling the nucleation and growth of plagioclase at P < 100 MPa when most of the water dissolved in the melt abruptly exsolves (Fig. 6). This leads to the conclusion that the plumbing system is characterized by the continuous supply of deeper, primitive magmas that mix with shallower, more differentiated ones. The degree of mixing is controlled by the magma supply rate at depth where different segments of the plumbing system may host compositionally distinct magmas. However, most of the crystallization is driven by decompression and degassing during magma ascent to the surface. In this frame, fractionation, mixing and degassing processes closely interact from mantle depths, to the shallow feeding system, to the summit crater of the volcano.

References

Applegarth, L.J., Tuffen, H., James, M.R., Pinkerton, H., Cashman, K.V., 2013. Direct observations of degassing-induced crystallization in basalts. Geology 41, 243-246.

Armienti, P., Perinelli, C., Putirka, K.D., 2013. A new model to estimate deep-level magma ascent rates, with applications to Mt. Etna (Sicily, Italy). Journal of Petrology 54, 795-813.

Armienti, P., Tonarini, S., Innocenti, F., D'Orazio, M., 2007. Mount Etna pyroxene as tracer of petrogenetic processes and dynamics of the feeding system, in: Beccaluva, L. Bianchini, G., Wilson, M. (Eds.), Cenozoic Volcanism in the Mediterranean, Geological Society of America Special Papers 418, pp. 265-276.

Armienti, P., Tonarini, S., D'Orazio, M., Innocenti, F., 2004. Genesis and evolution of Mount Etna alkaline lavas: Petrological and Sr-Nd-B isotope constraints. Periodico di Mineralogia 73, 29-52.

Armienti, P., Pareschi, M.T., Pompilio, M., Innocenti, F., 1994a. Effects of magma storage and ascent on the kinetics of crystal growth: the case of the 1991-1993 Mt. Etna eruption, Contribution to Mineralogy and Petrology 115, 402-414.

Armienti, P., Clocchiatti, R., D'Orazio, M., Innocenti, F., Petrini, R., Pompilio, M., Tonarini, S., Villari, L., 1994b. The long-standing 1991–1993 Mount Etna eruption: petrography and geochemistry of lavas. Acta Vulcanologica 4, 15–28.

Brugger, C.R., Hammer, J.E., 2010. Crystallization kinetics in continuous decompression experiments: implications for interpreting natural magma ascent processes. Journal of Petrology 51, 1941-1965.

Cashman, K.V., 1993. Relationship between plagioclase crystallization and cooling rate in basaltic melts. Contribution to Mineralogy and Petrology 113, 126-142.

Clocchiatti, R., Condomines, M., Guènot, N., Tanguy, J.C., 2004. Magma changes at Mount Etna: the 2001 and 2002–2003 eruptions. Earth and Planetary Science Letters 226, 397-414.

Collins, S.J., Pyle, D.M., Maclennan, J., 2013. Melt inclusions track pre-eruption storage and dehydration of magmas at Etna. Geology 37, 571-574.

Corsaro, R.A., Miraglia, L., Pompilio, M., 2007. Petrological evidence of a complex plumbing system feeding the July-August 2001 eruption of Mt. Etna, Sicily, Italy. Bulletin of Volcanology 69, 401-421.

Corsaro, R.A., Metrich, N., Allard, P., Andronico, D., Miraglia, L., Fourmentraux, C., 2009. The 1974 flank eruption of Mount Etna: an archetype for deep dike-fed eruptions at basaltic volcanoes and a milestones in Etna's recent history. Journal of Geophysical Research 114, B07204, doi:10.1029/2008JB006013.

Corsaro, R.A., Di Renzo, V., Distefano, S., Miraglia, L., Civetta, L., 2013. Relationship between petrologic processes in the plumbing system of Mt. Etna and the dynamics of the eastern flank from 1995 to 2005. Journal of Volcanology and Geothermal Research 251, 75-89.

Danyushevsky, L.V., Plechov, P., 2011. Petrolog3: Integrated software for modeling crystallization processes. Geochemistry, Geophysics, Geosystems 12, Q07021.

Del Bello E., Mollo S., Scarlato P., von Quadt A., Forni F., Bachmann O., 2014. New petrological constraints on the last eruptive phase of the Sabatini Volcanic District (central Italy): Clues from mineralogy, geochemistry, and Sr–Nd isotopes. Lithos, 205, 28-38.

Dolfi, D., Trigila, R., 1983. Clinopyroxene solid solutions and water in magmas: results in the system phonolitic tephrite-H_2O. Mineralogical Magazine 47, 347-351.

Ferlito, C., Viccaro, M., Cristofolini, R., 2008. Volatile-induced magma differentiation in the plumbing system of Mt. Etna volcano (Italy): evidence from glass in tephra of the 2001 eruption, Bulletin of Volcanology 70, 455-473.

Ferlito, C., Viccaro, M., Nicotra, E., Cristofolini, R., 2011. Regimes of magma recharge on the eruptive behaviour during the period 2001-2005 at Mt. Etna volcano. Bulletin of Volcanology 74, 533-543.

Ferlito, C., Lanzafame, G., 2012. The role of supercritical fluids in the potassium enrichment of magmas at Mount Etna volcano (Italy). Lithos 119, 642-650.

Ferlito, C., Coltorti, M., Lanzafame, G., Giacomoni, P.P., 2014. The volatile flushing triggers eruptions at open conduit volcanoes: Evidence from Mount Etna volcano (Italy). Lithos 184-187, 447-455.

France, L., Ildefonse, B., Koepke, J., Bech, F. 2010. A new method to estimate the oxidation state of basaltic series from microprobe analyses. Journal of Volcanology and Geothermal Research 189, 340-346.

Ghiorso, M.S., Sack, R.O., 1995. Chemical mass-transfer in magmatic processes IV. A revised and internally consistent thermodynamic model for the interpolation and extrapolation of liquidus-solid equilibria in magmatic systems at elevated temperatures and pressures. Contribution to Mineralogy and Petrology 119, 197-212.

Giacomoni, P.P., Ferlito, C., Coltorti, M., Bonadiman, C., Lanzafame, G., 2014. Plagioclase as Archive of Magma Ascent Dynamics on "Open Conduit" Volcanoes: the 2001-2006 Eruptive Period at Mount Etna. Earth-Science Reviews, in press.

Iezzi, G., Mollo, S., Shaini, E., Cavallo, A., Scarlato, P., 2014. The cooling kinetics of plagioclase revealed by electron microprobe mapping. American Mineralogist 99, 898-907.

Jeffery, A.J., Gertisser, R., Troll, V.R., Jolis, E.M., Dahren, B., Harris, C., Tindle, A.G., Preece, K., O'Driscoll, B., Humaida, H., Chadwick, J.P., 2013. Magma plumbing system of the 2007–2008 dome-forming eruption of Kelut volcano, East Java, Indonesia. Contribution to Mineralogy and Petrology 166, 275-308.

Kahl, M., Chakraborty, S., Costa, F., Pompilio, M., 2013. Dynamic plumbing system beneath volcanoes revealed by kinetic modeling, and the connection to monitoring data: An example from Mt. Etna. Earth and Planetary Science Letters 308, 11-22.

Kahl, M., Chakraborty, S., Costa, F., Pompilio, M., Liuzzo, M., Viccaro, M., 2011. Compositionally zoned crystals and real-time degassing data reveal changes in magma transfer dynamics during the 2006 summit eruptive episodes of Mt. Bulletin of Volcanology 75, 1-14.

Kamenetsky, V., Clocchiatti, R., 1996. Primitive magmatism of Mt. Etna: insights from mineralogy and melt inclusions. Earth and Planetary Science Letters 142, 553-572.

Kamenetsky, V.S., Pompilio, M., Métrich, N., Sobolev, A.V., Kuzmin, D.V., Thomas, R., 2007. Arrival of extremely volatile-rich high-Mg magmas changes explosivity of Mount Etna, Geology 35, 255-258.

Kress, V.C., Carmichael, I.S.E., 1991. The compressibility of silicate liquids containing Fe_2O_3 and the effect of composition, temperature, oxygen fugacity and pressure on their redox states, Contribution to Mineralogy and Petrology 108, 82-92.

Lange, R.A., Frey, H.M., Hector, J., 2009. A thermodynamic model for the plagioclase-liquid hygrometer/thermometer. American Mineralogist 94, 494-506.

Lanzafame, G., Mollo, S., Iezzi, G., Ferlito, C., Ventura, G., 2013. Unraveling the solidification path of a pahoehoe "cicirara" lava from Mount Etna volcano. Bulletin of Volcanology 75, 1-16.

Metrich, N., Rutherford, M.J., 1998. Low pressure crystallization paths of H_2O-saturated basaltic-hawaitic melts from Mt Etna: implications for open-system degassing of basaltic volcanoes. Geochimica et Cosmochimica Acta 62, 1195-1205.

Métrich, N., Allard, P., Spilliaert, N., Andronico, D., Burton, M., 2004. 2001 flank eruption of the alkali- and volatile-rich primitive basalt responsible for Mount Etna's evolution in the last three decades. Earth and Planetary Science Letters 228, 1-17.

Michaud, V., 1995. Crustal xenoliths in recent hawaiites from Mount Etna, Italy: evidence for alkali exchanges during magma-wall rock interaction. Chemical Geology 122, 21-42.

Mollo, S., Del Gaudio, P., Ventura, G., Iezzi, G., Scarlato, P., 2010. Dependence of clinopyroxene composition on cooling rate in basaltic magmas: implications for Thermobarometry. Lithos 118, 302-312.

Mollo, S., Lanzafame, G., Masotta, M., Iezzi, G., Ferlito, C., Scarlato, P., 2011a. Cooling history of a dike as revealed by mineral chemistry: a case study from Mt. Etna volcano. Chemical Geology 288, 39-52.

Mollo, S., Putirka, K., Iezzi, G., Del Gaudio, P., Scarlato, P., 2011b. Plagioclase-melt (dis)equilibrium due to cooling dynamics: implications for thermometry, barometry and hygrometry. Lithos 125, 221-235.

Mollo, S., Scarlato, P., Lanzafame, G., Ferlito, C., 2013a. Deciphering lava flow post-eruption differentiation processes by means of geochemical and isotopic variations: A case study from Mt. Etna volcano. Lithos 162-163, 115-127.

Mollo, S., Putirka, K., Misiti, V., Soligo, M., Scarlato, P., 2013b. A new test for equilibrium based on clinopyroxene-melt pairs: Clues on the solidification temperatures of Etnean alkaline melts at post-eruptive conditions. Chemical Geology 352, 92-100.

Mollo, S., Blundy, J.D., Scarlato, P., Iezzi, G., Langone, A., 2013c. The partitioning of trace elements between clinopyroxene and trachybasaltic melt during rapid cooling and crystal growth. Contribution to Mineralogy and Petrology 166, 1633-1654.

Mollo, S., Putirka, K., Iezzi, G., Scarlato, P., 2013d. The control of cooling rate on titanomagnetite composition: Implications for a geospeedometry model applicable to alkaline rocks from Mt. Etna volcano. Contribution to Mineralogy and Petrology 165, 457-475.

Mollo, S., Masotta, M., 2014. Optimizing pre-eruptive temperature estimates in thermally and chemically zoned magma chambers. Chemical Geology 368, 97-103.

Moore, G.M., Vennemann, T., Carmichael, I.S.E., 1995. Solubility of water in magmas to 2 kbar, Geology 23, 1099-1102.

Moore, G.M., Carmichael, I.S.E., 1998. The hydrous phase equilibria (to 3 kbar) of an andesite and basaltic andesite from Western Mexico: constraints on water content and conditions of phenocryst growth. Contribution to Mineralogy and Petrology 130, 304-319.

Nicotra, E., Viccaro, M. 2012. Unusual magma storage conditions at Mt. Etna (Southern Italy) as evidenced by plagioclase megacryst-bearing lavas: implications for the plumbing system geometry and summit caldera collapse. Bulletin of Volcanology 74, 795-825.

Patanè, D., De Gori, P., Chiarabba, C., Bonaccorso, A., 2003. Magma ascent and the pressurisation of Mount Etna's volcanic system. Science 299, 2061-2063.

Putirka, K., Johnson, M., Kinzler, R., Walker, D., 1996. Thermobarometry of mafic igneous rocks based on clinopyroxene–liquid equilibria, 0–30 kbar. Contribution to Mineralogy and Petrology 123, 92-108.

Putirka, K., 2008. Thermometers and barometers for volcanic systems, in Putirka, K.D., Tepley, F. (Eds.), Minerals, inclusions and volcanic processes. Reviews in mineralogy and geochemistry 69, pp. 61-120.

Roeder, P.L., Emslie, R.F., 1970. Olivine–liquid equilibrium. Contribution to Mineralogy and Petrology 29, 275-289.

Scarlato P., Mollo, S., Blundy, J.D., Iezzi, G., Tiepolo, M., 2014. The role of natural solidification paths on REE partitioning between clinopyroxene and melt. Bulletin of Volcanology 76, 1-4.

Schiano P., Clocchiatti, R., Ottolini, L., Sbrana, A., 2004. The relationship between potassic, calc-alkaline and Na-alkaline magmatism in South Italy volcanoes: A melt inclusion approach. Earth and Planetary Science Letters 220, 121-137.

Shea, T., Hammer, J.E., 2013. Kinetics of decompression and cooling-induced crystallization of mafic-intermediate hydrous magmas. Journal of Volcanology and Geothermal Research 260, 127-145.

Sisson, T.W., Grove, T.L., 1993. Experimental investigations of the role of H_2O in calcalkaline differentiation and subduction zone magmatism. Contribution to Mineralogy and Petrology 113, 143-166.

Spencer, K.J., Lindsley, D.H., 1981. A solution model for coexisting iron-titanium oxides. American Mineralogist 66, 1189-1201.

Spilliaert, N., Allard, P., Metrich, N., Sobolev, A.V., 2006. Melt inclusion record of the conditions of ascent, degassing, and extrusion of volatile-rich alkali basalt feeding the powerful 2002 flank eruption of Mount Etna (Italy). Journal of Geophysical Research 111, B04203.

Tanguy, J.C., Crocchiati, R., 1984. The Etnean lavas, 1977-1983: petrology and mineralogy. Bulletin of Volcanology 47, 879-894.

Tanguy, J.C., Condomines, M., Kieffer, G., 1997. Evolution of the Mount Etna magma: constraints on the present feeding system and eruptive mechanism. Journal of Volcanology and Geothermal Research 75, 221-250.

Vetere, F., Iezzi, G., Behrens, H., Cavallo, A., Misiti, V., Dietrich, M., Knipping, J., Ventura, G., Mollo, S., 2013. Intrinsic solidification behaviour of basaltic to rhyolitic melts: A cooling rate experimental study. Chemical Geology, 354: 233-242.

Viccaro, M., Cristofolini, R., 2008. Nature of mantle heterogeneity and its role in the short-term geochemical and volcanological evolution of Mt. Etna (Italy). Lithos 105, 272-288.

Viccaro, M., Ferlito, C., Cortesogno, L., Cristofolini, R., Gaggero, and L., 2006. Magma mixing during the 2001 event at Mt. Etna (Italy): effects on the eruptive dynamics. Journal of Volcanology and Geothermal Research 149, 139-159.

Viccaro, M., Giacomoni, P.P., Ferlito, C., Cristofolini, R., 2010. Dynamics of magma supply at Mt. Etna volcano (Southern Italy) as revealed by textural and compositional features of plagioclase phenocrysts. Lithos 116, 77-91.

Witham, F., Blundy, J.D., Kohn, S.C., Lesne, P., Dixon, J., Churakov, S.V., Botcharnikov, R., 2012. SolEx: a model for mixed COHSCl-volatile solubilities and exsolved gas compositions in basalt. Computer and Geosciences 45, 87-97.

Figure captions

Fig. 1. Comparison of natural, experimental and thermodynamic datasets recovered for olivine (a), clinopyroxene (b), plagioclase (c) and titanomagnetite (d) compositions. These datasets are reported in the Excel spreadsheet submitted as supplementary material. Fo = forsterite; Mg# = $Mg/(Mg+Fe^{2+})\times100$ moles; An = anorthite; Usp = ulvospinel. Dashed lines indicate that the

compositions of some experimental or thermodynamic phases were not provided for all major elements. For example, the thermodynamic code of Ghiorso and Sack (1995) does not account for the partitioning of Fe between plagioclase and melt.

Fig. 2. Results from MELTS simulations showing the relationship between the degree of melt differentiation (expressed as MgO wt.%) and the amount of fractionated solid in wt.%. MELTS data have been obtained by using as starting composition a more evolved $Mg\#_{50}$ trachybasalt equilibrated at 400 MPa (a) and 100 MPa (b), and a primitive $Mg\#_{63}$ basalt equilibrated at 400 MPa (c) and 100 MPa (d). Runs have been conducted by considering 1 and 2 wt.% H_2O in the system. The compositional range of recent 2001-2012 lavas is also displayed in figure as a grey field. ol = olivine; cpx = clinopyroxene; plg = plagioclase; timt = titanomagnetite.

Fig. 3 Test for equilibrium between clinopyroxene and melt based on the thermodynamic expression for diopside+hedenbergite (DiHd) of Mollo et al. (2013b) (a). Test for equilibrium between plagioclase and melt based on the Ab-An exchange reaction of Putirka (2008) (b). Estimate of the oxygen fugacity by the oxygen barometer of France et al. (2010) based on the different partitioning behaviour of ferrous and ferric iron between plagioclase, clinopyroxene, and melt (c). Test for equilibrium between olivine and melt based on the Fe-Mg exchange reaction of Roeder and Emslie (1970) (d).

Fig. 4. Temperature (a) and pressure (b) predictions of olivine crystallization obtained through the mineral-melt liquidus association option of Petrolog3 (Danyushevsky and Plechov, 2011). Temperature (c) and pressure (d) predictions of clinopyroxene crystallization derived by the pressure- and H_2O-independent thermometer of Putirka et al. (1996) and the liquid-independent barometer of Putirka (2008).

Fig. 5. P vs. H_2O estimates conducted with the clinopyroxene-based hygrometer of Armienti et al. (2013) show water contents in equilibrium with clinopyroxene as a function of pressure (a). The arrow represents the water decrease with decreasing pressure. Using the plagioclase-based hygrometer of Lange et al. (2009), we have also measured the water content in the melt at low pressures (b). Results are consistent with H_2O solubility values calculated through the computer program SolEx of Witham et al. (2011).

Fig. 6. Schematic representation of T-P paths driving the crystallization of magmas at Mt. Etna. Primitive basalts crystallize Mg-rich olivine and clinopyroxene at 600-1100 and 1150-1250 °C. Conversely, evolved trachybasaltic magmas equilibrate with Mg-poor mafic phenocrysts at 0.1-500 MPa and 1050-1175 °C. Most of the crystallization of plagioclase occurs at shallow levels and in the conduit due to the effect of water degassing and magma decompression.
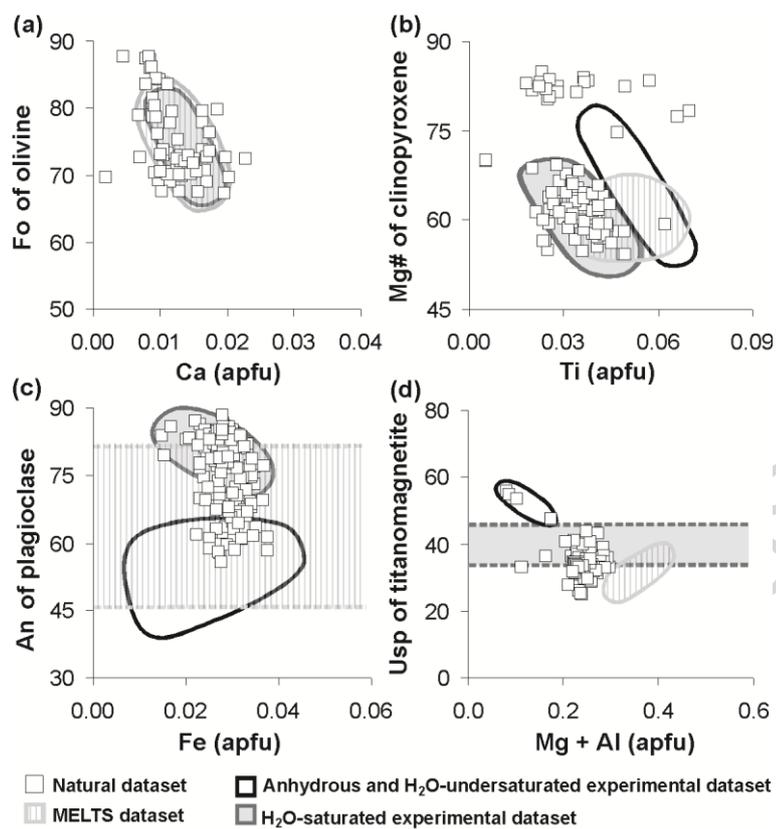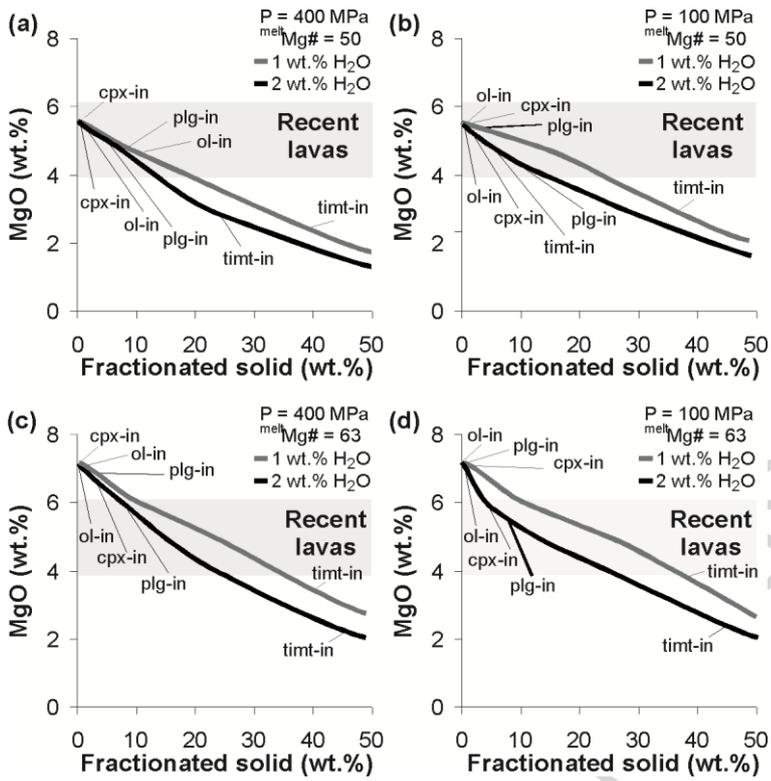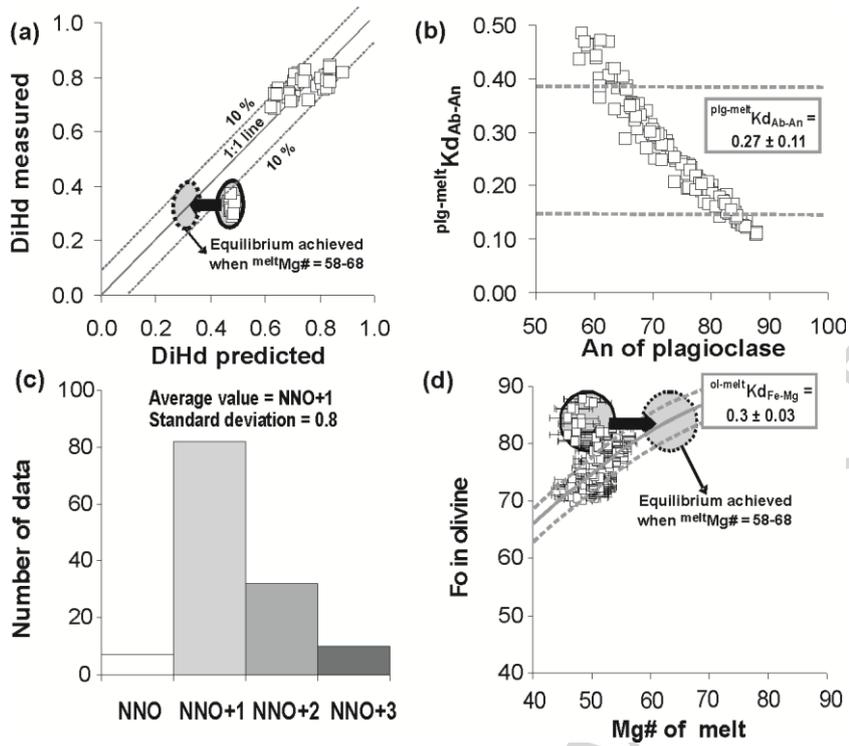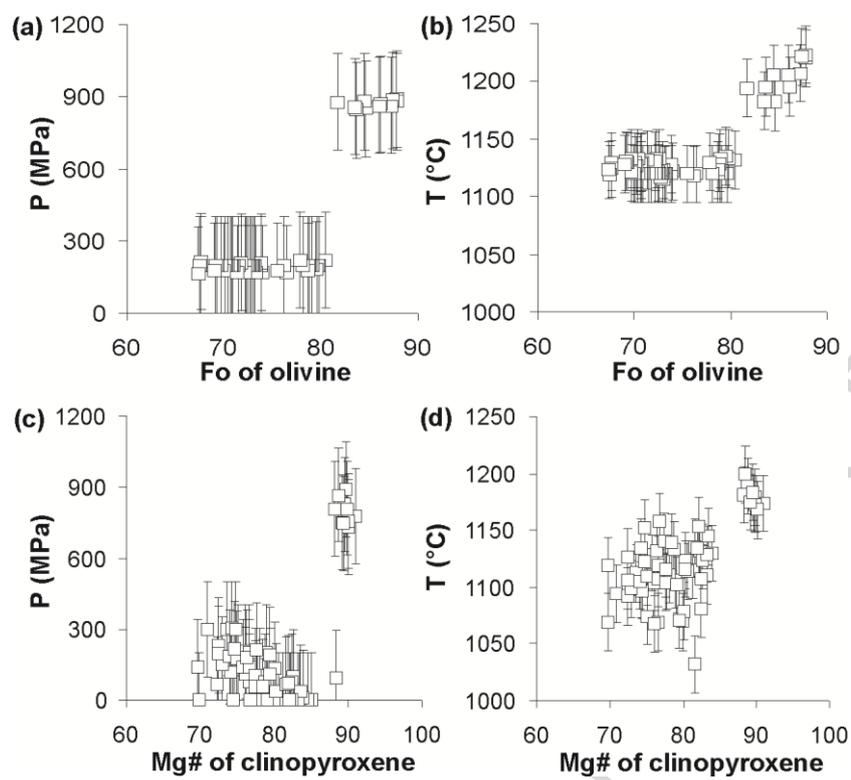
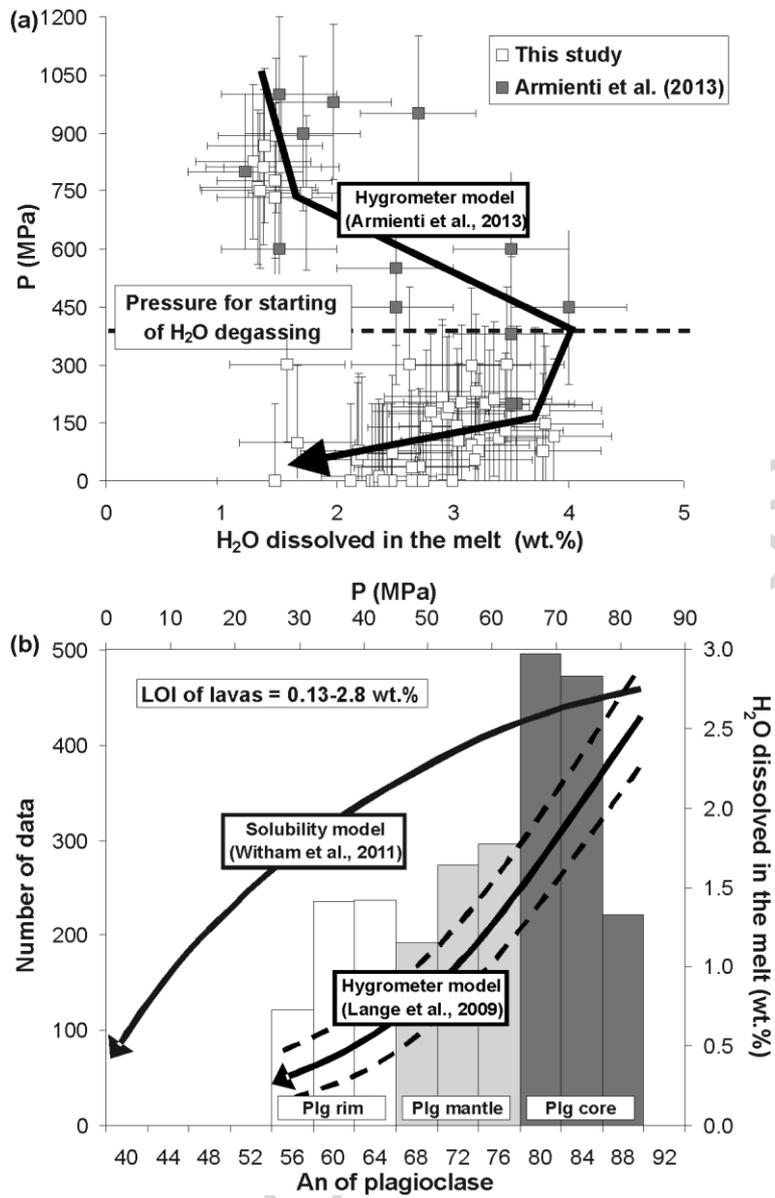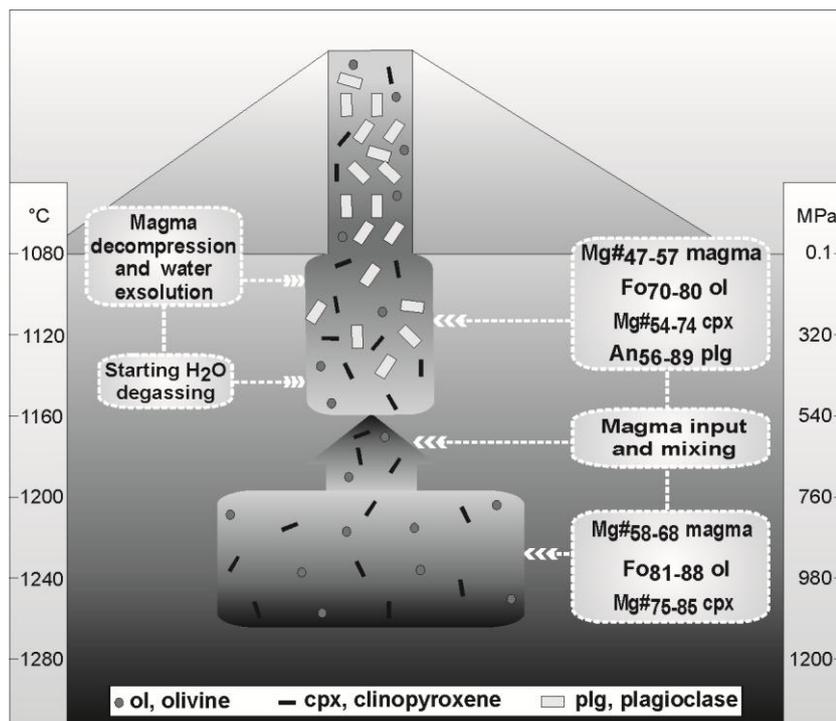Figure 1

Figure 2

Figure 3

Figure 4

Figure 5

Figure 6

Research Highlights

Mineral compositions at Mt. Etna are clear indicators of magma crystallization conditions. > Etnean magmas fractionate throughout the entire length of the vertically developed plumbing system. > Magma mixing, volatile exsolution and degassing are key processes driving eruptions.